Springer

Journal of
Mechanical
Science and
Technology

Journal of Mechanical Science and Technology 22 (2008) 269~275

www.springerlink.com/content/1738-494x

Mistuned coupling stiffness effect on the vibration localization of cyclic systems

Sang Ha Shin, Min Kyoo Kang and Hong Hee Yoo*

Department of Mechanical Engineering, Hanyang University 17 Haengdang-Dong Sungdong-Gu Seoul 133-791, Korea

(Manuscript Received April 16, 2007; Revised August 7, 2007; Accepted August 23, 2007)

Abstract

In cyclic structural systems, small property irregularities often cause significant differences in the dynamic responses of their subcomponents, which results in unpredicted premature failures of the systems. The small irregularities and the resulting phenomena are called the mistuning and the vibration localization, respectively. In this paper, the vibration localization phenomena due to mistuned coupling stiffness are investigated. For the investigation, a simple multi-pendulum system is employed and an optimization method is used to find mistuned coupling stiffness conditions under which maximum vibration localization phenomena occur.

Keywords: Mistuning; Cyclic system; Vibration; Localization; Coupling stiffness

1. Introduction

Cyclic structures, in which identical subcomponents are repeated, can be found in several engineering examples such as turbine and helicopter blades. Cyclic structures, however, are not perfectly periodic since there always exist slight mistuning (or disorders) due to manufacturing tolerances and material property irregularities. Furthermore, even a perfect cyclic structure could be deteriorated due to operation wear. The forced vibration responses of some subcomponents of a mistuned structure become often much larger than those of a perfectly tuned ideal structure. Vibration energy tends to concentrate on a few subcomponents of the mistuned cyclic structure. This phenomenon, which is called vibration localization, often causes unexpected premature failures of cyclic structures, so the effect of mistuning on the vibration localization needs to be investigated.

Since the pioneering work of Anderson [1] on localization in disordered periodic systems in solid-state physics, localization phenomena have drawn attention from many researchers in mechanical engineering. Ewins [2-4] showed that the maximal forced response increases as the mistuning increases up to certain level. However, further increase of mistuning results in lower forced response. Hodges [5] was the first to recognize the relevance of localization theory on dynamical behavior of periodic structures. Bendiksen [6] investigated mode localization of mistuned turbomachinery rotors using disordered chain of coupled pendulum. Pierre et al. [7] investigated mode localization of disordered multi-span beams and explained mode localization by perturbation method. Pierre et al. [8] also introduced intentional mistuning into bladed disk design in order to reduce the maximal forced response. Recently, Yoo et al [9] investigated localization phenomena by analyzing the forced vibration responses. They found a certain relation between subcomponent stiffness mistuning and coupling stiffness for localization. In this study, however, the coupling stiffness is assumed to have no mistuning and only small degrees of freedom examples were investigated.

The subcomponent stiffness of a cyclic structure is assumed mistuned, while the coupling stiffness was assumed tuned in the previous study. In the present study, the effect of mistuned coupling stiffness on the vibration localization is investigated. The subcompo-

*Corresponding author. Tel.: +82 2 2220 0446, Fax.: +82 2 2293 5070
E-mail address: hhyoo@hanyang.ac.kr
DOI 10.1007/s12206-007-1032-7

nent stiffness is assumed tuned, on the contrary. To consider more practical problems having large degrees of freedom, an optimization method that combines a genetic algorithm [10] along with a gradient-based search algorithm [11] is employed in the present study. Lastly, different from the previous study, the excitation force for each subcomponent of a cyclic structure is assumed to have different phase angle.

2. Simplified coupled cyclic model and an optimization problem

Cyclic structures have repeated subcomponents that have identical structural topology including geometry, stiffness, and damping. The mistuning of a cyclic structure may result from irregularities of material or geometric properties. Fig. 1 shows a planar system having n coupled pendulums. Each pendulum has a torsional spring of modulus k_r and two translational springs of modulus k_t. The distance from hinge point to translational springs is a. Even though damping symbols do not appear in Fig. 1, a linear viscous damping force (with damping constant c) is assumed to act on each pendulum mass. If each pendulum mass is excited by excitation force f^i, the equation of motion of the i-th pendulum is derived as follows:

$$\begin{aligned} & m^i \ \ l^2\ddot{\theta}^i + c^i \ \ l^2\dot{\theta}^i + k_r^i\theta^i - k_t^{i-1} \ \ a^2\theta^{i-1} \\ & +(k_t^{i-1}+k_t^i) \ \ a^2\theta^i - k_t^i \ \ a^2\theta^{i+1} = f^i \ \ l \end{aligned} \tag{1}$$

where l represents the length of pendulums. In this study, f^i's are assumed to be identical except the phase difference. The phase angle of the i-th pendulum ϕ_i is assumed to be equal to $2(i-1)\pi/n$. Such phase angle is realistic in many cases since the excitation force for each subcomponent is serially applied. Turbine nozzle excitation force is a typical example.

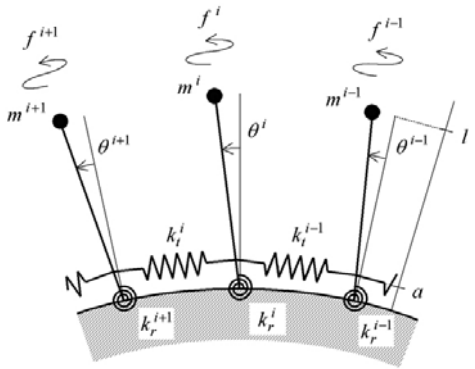

Fig. 1. Multiple coupled pendulum system.

Assuming tuned properties of mass m, damping constant c, and torsional spring modulus k_r, Eq. (1) can be written as follows:

$$\begin{aligned} & m \ \ l^2\ddot{\theta}^i + c \ \ l^2\dot{\theta}^i + k_r\theta^i - k_t^{i-1} \ \ a^2\theta^{i-1} \\ & +(k_t^{i-1}+k_t^i) \ \ a^2\theta^i - k_t^i \ \ a^2\theta^{i+1} = f \ \ l \ \ e^{j\phi_i} \end{aligned} \tag{2}$$

To obtain more general and useful conclusions from the equation of motion, dimensionless parameters and a dimensionless variable are defined as follows:

$$\begin{aligned} & \beta_i \equiv \frac{k_t^i \ \ a^2}{k_r} \ , \quad \varsigma \equiv \frac{cl}{2\sqrt{k_r m}} \ , \\ & \gamma \equiv \frac{f \ \ l}{k_r} \ , \quad \tau \equiv \sqrt{\frac{k_r}{ml^2}} \ \ t \end{aligned} \tag{3}$$

where β_i represents coupling stiffness between subcomponents, ς represents damping, γ represents external force, and τ represents a normalized time. In this study, these dimensionless parameters are only used for numerical analysis. Employing these dimensionless parameters and variable, Eq. (2) can be rewritten as follows:

$$\begin{aligned} & \ddot{\theta}^i + 2\zeta\dot{\theta}^i - \beta_{i-1} \ \ \theta^{i-1} \\ & +(1+\beta_{i-1}+\beta_i) \ \ \theta^i - \beta_i\theta^{i+1} = \ \ \gamma e^{j\phi_i} \end{aligned} \tag{4}$$

where a dotted symbol represents the differentiation of the symbol with respect to dimensionless time variable τ. Therefore, the equations of motion can be written as follows:

$$[M]\{\ \ddot{\theta}\ \} + 2\varsigma[M]\{\ \dot{\theta}\ \} + [K]\{\ \theta\ \} = \gamma\{F\} \tag{5}$$

where

$$[M] = \begin{bmatrix} 1 & 0 & \cdots & \cdots & 0 \\ 0 & \ddots & \ddots & \ddots & \vdots \\ \vdots & \ddots & 1 & \ddots & \vdots \\ \vdots & \ddots & \ddots & \ddots & 0 \\ 0 & \cdots & \cdots & 0 & 1 \end{bmatrix} \quad \{\ \theta\} = \begin{Bmatrix} \theta^1 \\ \vdots \\ \theta^i \\ \vdots \\ \theta^n \end{Bmatrix} \quad \{F\} = \begin{Bmatrix} e^{j\phi_1} \\ \vdots \\ e^{j\phi_i} \\ \vdots \\ e^{j\phi_n} \end{Bmatrix}$$

$$[K] = \begin{bmatrix} 1+\beta_n+\beta_1 & -\beta_1 & 0 & 0 & -\beta_n \\ -\beta_1 & \ddots & \ddots & 0 & 0 \\ 0 & -\beta_{i-1} & 1+\beta_{i-1}+\beta_i & -\beta_i & 0 \\ 0 & 0 & \ddots & \ddots & -\beta_{n-1} \\ -\beta_n & 0 & 0 & -\beta_{n-1} & 1+\ \beta_{n-1}+\beta_n \end{bmatrix} \tag{6}$$

Taking Fourier transformation of Eq. (5) yields the following matrix equation.

$$\left(-\omega^2[M]+j2\varsigma\omega[M]+[K]\right)\{\bar{\theta}\}=\bar{\gamma}\{F_x+jF_y\} \tag{7}$$

where $\{\bar{\theta}\}$ and $\bar{\gamma}$ are the Fourier transformations of $\{\theta\}$ and γ respectively, F_x^i is $\cos\phi^i$, and F_y^i is $\sin\phi^i$. Now, from Eq. (7), one can obtain $\{\bar{\theta}\}$ which represents the frequency response of the pendulum system. Substituting $\bar{\theta}_i = X_i + jY_i$ into Eq. (7), the following equation can be derived.

$$\begin{bmatrix} -\omega^2[M]+[K] & -2\ \varsigma\omega\ [M] \\ 2\varsigma\ \omega\ [M] & -\omega^2[M]+[K] \end{bmatrix}\begin{Bmatrix}\{X\}\\ \{Y\}\end{Bmatrix}=\bar{\gamma}\begin{Bmatrix}\{F_x\}\\ \{F_y\}\end{Bmatrix} \tag{8}$$

To obtain X_i and Y_i from Eq. (8), a constant value for $\bar{\gamma}$ is employed since the excitation force is assumed to be a white noise. $\bar{\gamma}$, however, may be given differently if its frequency characteristics are known to the analyzer. The input parameters in this equation are the coupling stiffness β_i's. The output index is the maximum of $|\bar{\theta}_i|$, which will be denoted as κ_i hereinafter (see, Ref. [9]).

If the input parameters are given in Eq. (8), then the output index κ_i can be calculated. However, as the number of input parameters increases, the computational effort to find κ_i increases exponentially. So, to find the output index efficiently, an optimization method needs to be employed. To find global optimums in this problem, an optimization method that combines a genetic algorithm along with a gradient-based search algorithm [11] is employed to solve the problem. For the problem, design variables, the objective function, and constraints are given as follows:

Design variables: Dimensionless coupling parameters $\beta_i's$

Objective function: Minimize(-max(κ_i))

Side Constraints: $0.0 \le \beta_i \le 1.0$ ($i = 1, 2, \ldots, n$)

where max(κ_i) represents the maximum value among $\kappa_i's$. So, the maximum of max(κ_i) is actually to be found in this problem.

3. Numerical results and discussion

As mentioned in the previous section, the maximum of max(κ_i) and the corresponding design variables $\beta_i's$ are to be found in this section. The damping parameter ς is fixed to 0.005 and the phase difference ($\Delta\phi = \phi_i - \phi_{i-1}$) between two adjacent excitation forces is $2\pi/n$ when the system consists of n pendulums. While a turbine rotates, its nozzle excites the blades serially; thus, the phase difference emulates the nozzle excitation force acting on the blades.

Fig. 2 shows the variation of the max(κ_i) versus β_{tuned}, which is the tuned coupling stiffness. Since no mistuning is assumed in order to obtain the results, all $\beta_i's$ are identical, and so $\kappa_i's$ are identical, too. As shown from the figure, the max(κ_i) is 100 when β_{tuned} is equal to 0, which means no coupling between pendulums. The max(κ_i) decreases monotonically as the tuned coupling stiffness β_{tuned} increases. The decreasing rate, however, is attenuated as the number of pendulums increases.

Fig. 3 shows the variations of $\kappa_i's$ versus $\beta_i's$ for a 3-pendulum system. To obtain this figure, β_1 and β_2 vary independently while β_3 is fixed to 0.001. As shown from the figure, each κ_i reaches its maximum with a different combination of $\beta_i's$. When one of $\kappa_i's$ gets larger, the other κ_i gets smaller. Thus, the kinetic energy tends to concentrate on one of the pendulums of the mistuned system. The maximum of some κ_i reaches 116 which is larger than the tuned maximum response 100 (shown in Fig. 2). Thus, the mistuning results in a significant difference between the maximum dynamic responses of a tuned system and a mistuned system.

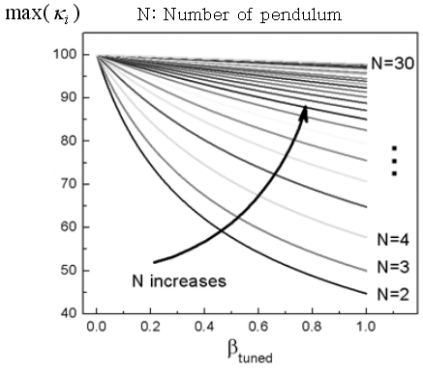

Fig. 2. Maximum response versus the tuned coupling stiffness.

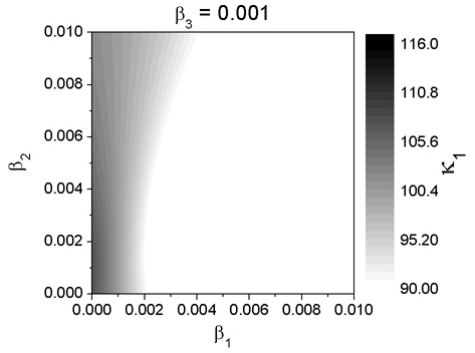

(a) Variation of κ_1

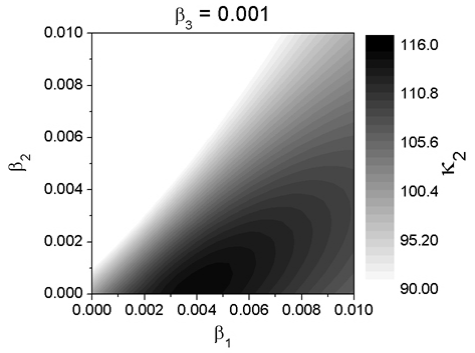

(b) Variation of κ_2

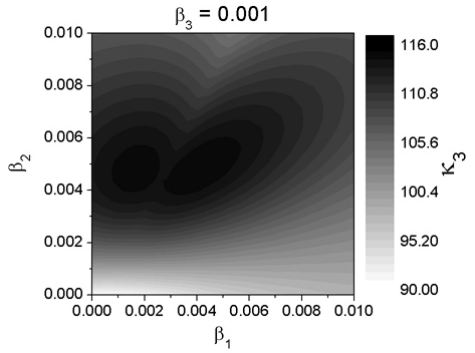

(c) Variation of κ_3

Fig. 3. Variations of κ_i's versus β_i's for a 3-pendulum system.

Fig. 4 now shows max(κ_i) versus β_i's. To obtain the maximum of max(κ_i) of the 3-pendulum system by using an exhaustive search method, it takes almost 36 hours with a pentium-4 personal computer. As the number of pendulums increases, the computing time increases exponentially. So, it is almost impossible to find the maximum value for systems having more than three pendulums by using an exhaustive search method. Therefore, one should rely on an

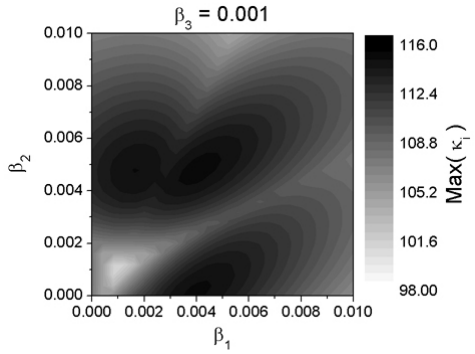

Fig. 4. Variation of max(κ_i) versus β_i's for a 3-pendulum system.

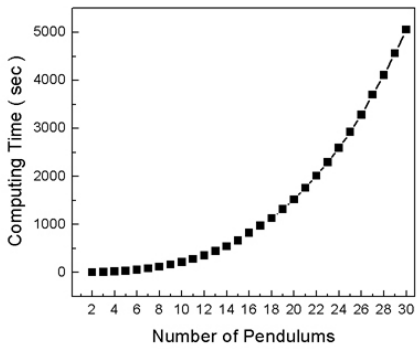

Fig. 5. Variation of computing time versus the number of pendulums.

efficient optimization method to find the solution efficiently. However, as shown in Fig. 4, several local maximums exist in max(κ_i). Therefore, a global optimization algorithm needs to be employed to avoid obtaining one of local maximums. In this study, a hybrid method that combines a genetic algorithm along with a gradient-based search algorithm is employed to find the maximum mistuned responses.

Fig. 5 shows the variation of computing time (versus the number of pendulums) that is obtained by using the optimization method. As shown from the figure, the computing time increases parabolically, instead of exponentially, as the number of pendulums increases. Even for the 30-pendulum system, the computing time is now in a reasonable range.

Fig. 6 shows the variation of the maximum of max(κ_i) versus the number of pendulums. All β_i's are chosen as design variables for the optimization problem. As shown in the figure, the maximum increases as the number of pendulums increases. In other words, the localization effect due to mistuned coupling stiffness increases as the number of pendu-

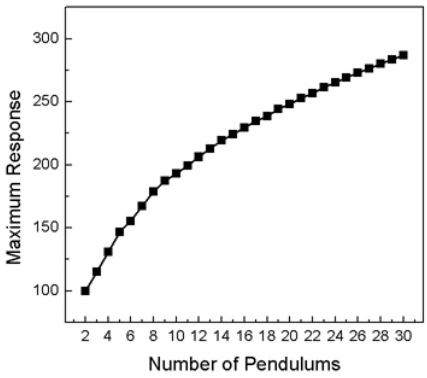

Fig. 6. Variation of maximum response versus the number of pendulums.

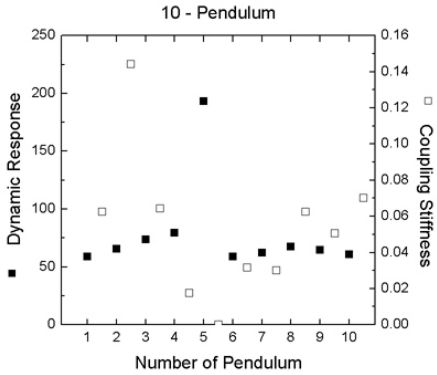

(a) Dynamic response and coupling stiffness

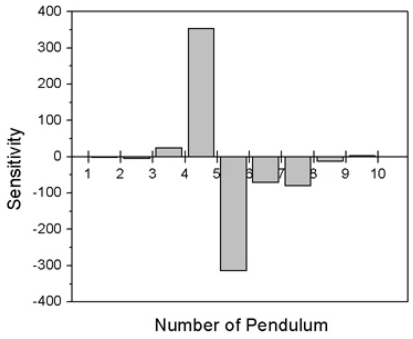

(b) Sensitivity

Fig. 7. Dynamic responses, coupling stiffness parameters, and the sensitivities of the solution obtained through optimization for a 10-pendulum system.

lums increases. The increasing rate, however, is attenuated as the number of pendulums increases. The maximum seems to be approximately proportional to the square root of the number of pendulums.

Figs. 7-9 show the maximum of max(κ_i), the corresponding coupling stiffness parameters β_i's, and

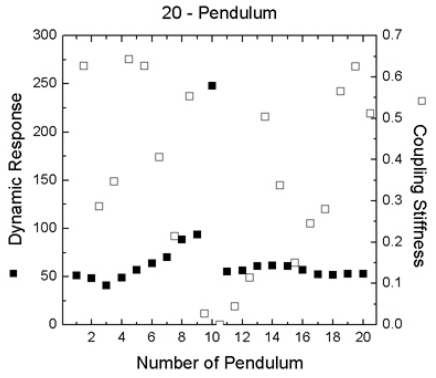

(a) Dynamic response and coupling stiffness

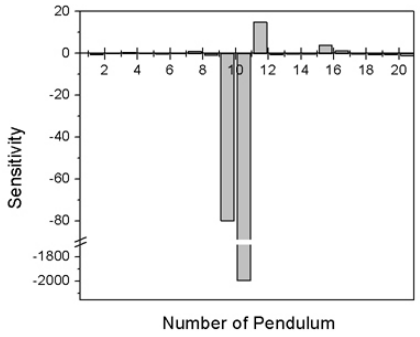

(b) Sensitivity

Fig. 8. Dynamic responses, coupling stiffness parameters, and the sensitivities of the solution obtained through optimization for a 20-pendulum system.

the sensitivity of the parameters. The results of three mistuned systems (having 10, 20 and 30 pendulums) are given in the figures, respectively. It can be observed that the maximum response always occurs at a pendulum that is located between two smallest coupling stiffness parameters. Also, the sensitivities of the two smallest coupling parameters are dominant over those of the rest of the coupling stiffness parameters. These results were obtained by using the formulation (for optimization) given in the previous section.

Since the two smallest coupling stiffness parameters of the solutions obtained through optimization are dominantly sensitive, their exact values are only employed while the other coupling stiffness parameters are assumed to vary identically. Since the rest of the coupling stiffness parameters, other than the two smallest ones, in Figs. 7-9 are little sensitive, they hardly influence the maximum of κ_i's. Fig. 10 shows the maximum of max(κ_i) versus the identically varied coupling stiffness and the number of

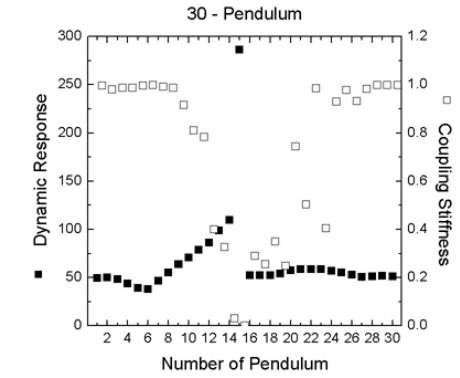

(a) Dynamic response and coupling stiffness

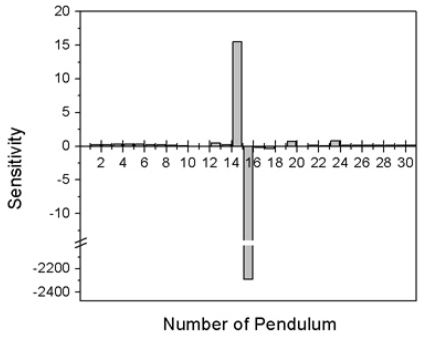

(b) Sensitivity

Fig. 9. Dynamic responses, coupling stiffness parameters, and the sensitivities of the solution obtained through optimization for a 30-pendulum system.

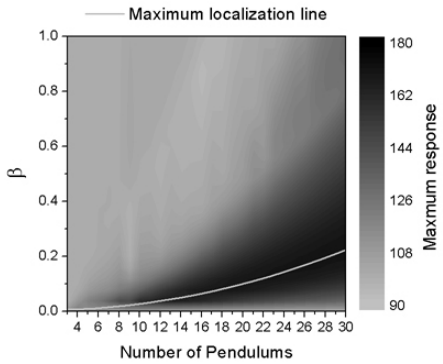

Fig. 10. Maximum response versus the identical coupling stiffness parameter and the number of pendulums.

pendulums. Note that the results of Fig. 2 and Fig. 10 have different tendency. For tuned systems, as the number of pendulums increases, the variation of the identical coupling stiffness little affects the maximum of κ_i's . However, for mistuned systems, the variation of the identical coupling stiffness still affects the maximum of κ_i's significantly even if the number of pendulums increases. As the number of pendulums increases, the maximum strength of the localization increases along the white line shown in Fig.10. The white line can be approximately represented by a parabolic equation between the coupling stiffness and the number of pendulums.

4. Conclusion

The mistuning effect of coupling stiffness on the vibration localization is investigated in this study. To deal with realistic problems having a large number of degrees of freedom, an optimization method that combines a genetic algorithm along with a gradient-based search algorithm is employed. The results show that the vibration localization gets stronger as the number of degrees of freedom increases. The solutions obtained through optimization also show that the maximum response occurs between two adjacent coupling springs having the smallest values. If the two smallest stiffness values of the two coupling springs are employed while the stiffness values of the rest of springs are assumed to vary identically, strong vibration localization may still occur. The maximum strength of the localization occurs along a parabolic line that relates the number of pendulums and the coupling stiffness.

Acknowledgments

This research was supported by Innovative Design Optimization Technology Engineering Research Center through research fund, for which authors are grateful.

References

[1] P. W. Anderson, Absence of diffusion in certain random lattices. *Physical Review* 109 (5) (1958) 1492-1505.

[2] D. J. Ewins, The effect of detuning upon the forced vibrations of bladed disks. *Journal of Sound and Vibration* 9 (1) (1969) 65-79.

[3] D. J. Ewins, Vibration characteristics of bladed disc assemblies, *Journal of Mechanical Engineering Science* 15 (3) (1973) 165-186.

[4] D. J. Ewins, Vibration modes of mistuned bladed disks, *ASME Journal of Engineering for Power* 98 (7) (1976) 349-355.

[5] C. H. Hodges, Confinement of vibration by structural irregularity, *Journal of Sound and Vibration* 82 (3) (1982) 411-424.

[6] O. O Bendiksen, Flutter of mistuned turboachinery rotors, *Journal of Engineering for Gas Turbines and Power* 106 (1) (1984) 25-33.

[7] C. Pierre, D. M. Tang and E. H. Dowell, Localized vibrations of disordered multispan beams: theory and experiment. *AIAA Journal,* 25 (9) (1987) 1249-1257.

[8] P. Castanier and C. Pierre, Consideration on the benefits of intentional blade mistuning for the forced response of turbomachinery rotors, *Analysis and Design Issues for Modern Aerospace Vehicles* 55 (1997) 419-425.

[9] H. H. Yoo, J. Y. Kim and D. J. Inman, Vibration localization of simplified mistuned cyclic structures undertaking external harmonic force, *Journal of Sound and Vibration,* 261 (5) (2003) 859-870.

[10] D. E. Goldberg, Genetic algorithms in search, optimization and Machine learning, *Addison Wesley Longman*, Inc. 1989.

[11] G. N. Vanderplaats, DOT-design optimization tools user manual, *Vanderplaats Research & Development*, Inc. (1999).